Journal of Alloys and Compounds 530 (2012) 107–110

Contents lists available at SciVerse ScienceDirect

Journal of Alloys and Compounds

journal homepage: www.elsevier.com/locate/jallcom

Preparation of room temperature ferromagnetic $BiFeO_3$ and its application as an highly efficient magnetic separable adsorbent for removal of Rhodamine B from aqueous solution

Jun Zhang[a], M.A. Gondal[b], Wei Wei[a], Taona Zhang[a], Qingyu Xu[c,d,**], Kai Shen[a,*]

[a] College of Materials Science and Technology, Nanjing University of Aeronautics and Astronautics, Nanjing 211100, China
[b] Physics Department and Center of Excellence in Nanotechnology, King Fahd University of Petroleum and Minerals, Dhahran 31261, Saudi Arabia
[c] Department of Physics, Southeast University, Nanjing 211189, China
[d] Key Laboratory of MEMS of the Ministry of Education, Southeast University, Nanjing 210096, China

ARTICLE INFO

Article history:
Received 10 January 2012
Received in revised form 12 March 2012
Accepted 17 March 2012
Available online 1 April 2012

Keywords:
$BiFeO_3$
Adsorption
Rhodamine B
Ferromagnetic

ABSTRACT

In this work, room temperature ferromagnetic $BiFeO_3$ ceramics has been prepared through complex-assisted sol–gel method by using tartaric acid as a complex and tested for the efficient adsorption removal of the model compound (Rhodamine B, RhB). The excellent adsorption property of RhB over as-prepared magnetic separable $BiFeO_3$ ceramics has been proved by batch adsorption experiments. Further studies indicate the static-electric adsorption mechanism may play an important role in the adsorption process. This is a first study of its kind where magnetic separable $BiFeO_3$ has been employed for efficient removal of RhB molecules from an aqueous solution.

1. Introduction

Perovskite type Bismuth ferrite ($BiFeO_3$), a rhombohedrally distorted cell with the polar R3c space group, is an excellent multiferroic material which exhibits simultaneously ferroelectric and antiferromagnetic ordering with relatively high Néel and Curie points (T_C ~1103 K, T_N ~643 K) [1,2]. The electrical, magnetic and optical properties of $BiFeO_3$ have been studied intensively in various applications such as RT magneto-electric devices and ferroelectric ultrafast optoelectronic devices [3–5].

Recently, the environmental applications in waste water treatment (specially the removal of dyes) using $BiFeO_3$ gradually attracted the attention of researchers due to its unique properties such as the weak ferromagnetic order at room temperature and allowing it to be recycled easily from aqueous solution [6]. The water contamination by organic pollutants like dyes is of great concern worldwide because of their utilization in different industrial processes. In early 2007, $BiFeO_3$ nanoparticles were reported as an active photocatalyst to decompose methyl orange, owning to the small band gap and appropriate valence band edge and therefore $BiFeO_3$ semiconductor plays an important role in the photocatalytic activity [7]. Thereafter, the photocatalytic degradation of dye molecules over $BiFeO_3$ with various morphologies were investigated [8–11]. More recently, the $BiFeO_3$ was demonstrated as an efficient Fenton-like heterogeneous catalyst to decompose dye molecules [12].

To the best of our knowledge, no data on the adsorption removal performance of Rhodamine B (RhB) dye over magnetic $BiFeO_3$ catalyst has been reported till date. In this investigation, the efficient adsorption removal of RhB (which is considered a toxic organic pollutant) is reported for the first time. The adsorption kinetics, isotherm and thermodynamic studies toward removal of RhB were systematically studied through batch adsorption experiments. The possible adsorption mechanism is discussed for the first time and reported in this work.

2. Experimental

2.1. Chemical reagents

The following chemicals, $Bi(NO_3)_3{\cdot}5H_2O$, $Fe(NO_3)_3{\cdot}9H_2O$, tartaric acid ($C_4H_6O_6$), nitric acid and model compound RhB dyes ($C_{28}H_{31}ClN_2O_3$) were used as received. All the commercial reagents were of analytical grade and used as received without further purification.

2.2. Preparation of Perovskite-type $BiFeO_3$

Perovskite-type $BiFeO_3$ ceramics were fabricated by a traditional sol–gel method. In a typical preparation, $Bi(NO_3)_3{\cdot}5H_2O$ and $Fe(NO_3)_3{\cdot}9H_2O$ were

* Corresponding author. Tel.: +86 25 8489 5871; fax: +86 25 8489 5871.
** Co-corresponding author.
E-mail addresses: xuqingyu@seu.edu.cn (Q. Xu), shenkai84@nuaa.edu.cn (K. Shen).

0925-8388/$ – see front matter.
http://dx.doi.org/10.1016/j.jallcom.2012.03.104

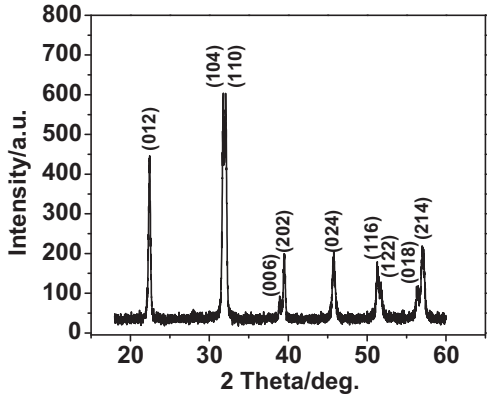

Fig. 1. XRD pattern of as-prepared perovskite-type $BiFeO_3$.

completely dissolved in distilled water in proper stoichiometric proportion. After being stirred for 2 h, tartaric acid was added to the solution mentioned above to afford a clear solution in which the mole ratio of $Bi(NO_3)_3{\cdot}5H_2O/Fe(NO_3)_3{\cdot}9H_2O$/tartaric acid was fixed at 1:1:2. The stable gels were obtained after stirring at 333 K for 5 h followed by heating at 413 K in the oven for 48 h. Calcination of the prepared gels was carried out in a tubular furnace at 600 °C for 2 h under air flow at atmospheric pressure to obtain the finial product of $BiFeO_3$ ceramics.

2.3. Characterization and magnetic property

The transmission electron microscopy (TEM) images were taken on a FEI Tecnai G2 20 S-TWIN TEM. The X-ray diffraction (XRD) patterns of the $BiFeO_3$ adsorbent before and after RhB adsorption were obtained by using a Bruker D8 ADVANCE X-ray powder diffractometer, using CuKα radiation (λ = 0.15418 nm) as the X-ray source. The magnetic property of the $BiFeO_3$ at room temperature was investigated by Physical Property Measurement System (PPMS).

2.4. Batch adsorption experiments

Batch adsorption experiments were conducted to examine the adsorption isotherm, adsorption kinetics, as well as the effect of solution pH and temperature on the adsorption process. The effect of pH on adsorption kinetics and isothermals was carried out in a constant temperature incubator shaker and the flasks were shaken at 150 rpm at room temperature. The effect of temperature on adsorption kinetics was conducted in a stirred water bath.

The pseudo-second-order model are adopted to determine RhB dye adsorption kinetics which is defined by

$$\frac{t}{q_t} = \frac{1}{k_2 q_e^2} + \frac{t}{q_e} \quad (1)$$

where q_t (mg g^{-1}) is the adsorption capacity at specific contact time, k_2 (g mg^{-1} h^{-1}) the pseudo-2nd-order kinetic constant and q_e (mg g^{-1}) the amount of RhB adsorbed on $BiFeO_3$ at equilibrium[13].

The most common adsorption isotherm models known as Langmuir and Freundlich isotherm models were adopted to fit the equilibrium adsorption data. The Langmuir isotherm theory assumes that the sorption takes place at specific homogeneous sites within the adsorbent, i.e. once an adsorbate molecule occupies a site, no further adsorption can take place at that site. Another basic assumption considered was that there is no interaction between the adsorbate molecules on the surface of the sorbent:

$$q_e = \frac{K_L q_m C_e}{1 + K_L C_e} \quad (2)$$

where C_e is the equilibrium concentration (mg L^{-1}), q_e the amount of adsorbate adsorbed (mg g^{-1}), Q_0 the theoretical monolayer capacity (mg g^{-1}), and K_L is the adsorption equilibrium constant (L mg^{-1}) [14].

The Freundlich isotherm is the earliest known relationship describing the adsorption equation. It assumes that as the adsorbate concentration in solution increases so too does the concentration of adsorbate on the adsorbent surface and therefore, has an exponential expression:

$$q_e = K_F C_e^{1/n} \quad (3)$$

where K_F and n are the Freundlich constants representing the adsorption capacity and the adsorption intensity, respectively [14].

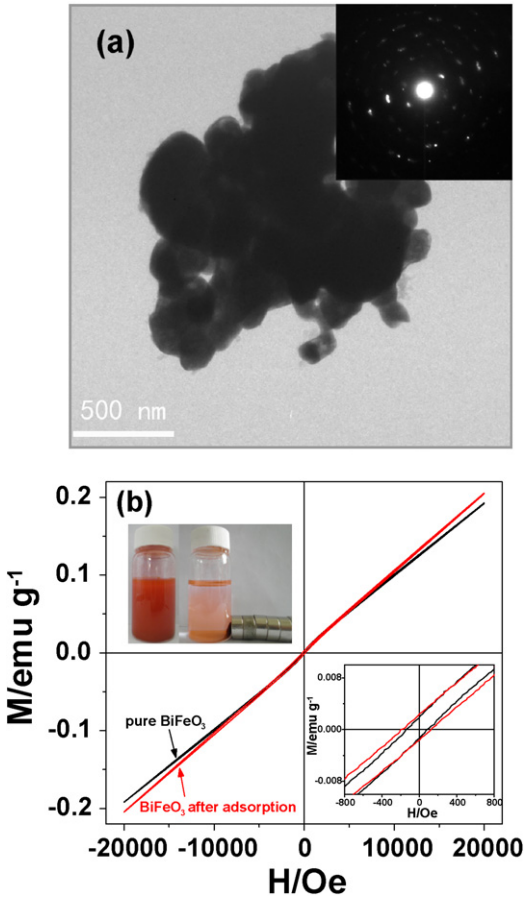

Fig. 2. TEM images (a) of as-prepared $BiFeO_3$ adsorbent (inset shows the SAED pattern) and M–H hysteresis loops (b) for the $BiFeO_3$ measured at room temperature (the inset on the lower right depicts the partially enlarged curve, and the inset on the left top show the $BiFeO_3$ can be well-dispersed in aqueous solution (left) and magnetic separated by an external magnetic field (right)). (For interpretation of the references to color in text, the reader is referred to the web version of the article.)

3. Results and discussion

The XRD result confirms the single phase perovskite structure of as prepared $BiFeO_3$ sample which is depicted in Fig. 1. It can be observed that all of the diffraction peaks can be indexed to the rhombohedral structure of $BiFeO_3$ (JCPDS No. 71-2494) with fine crystallinity. TEM was employed to investigate the crystal morphology of the as-synthesized $BiFeO_3$. As depicted in Fig. 2(a), the Bright-Field (BF) image which were recorded by means of a small objective aperture which selected only the (0 0 0) central transmitted beam, suggested the particle size is in the range of 300–500 nm. The ring-pattern in SAED (inset) clearly indicates the polycrystalline structure of as-prepared $BiFeO_3$ sample. To date, perovskite-type $BiFeO_3$ has been well known to be one of the several materials exhibiting ferromagnetic properties at room temperature [7]. The coercive values of as-prepared bulk $BiFeO_3$ and $BiFeO_3$ after adsorption were examined at around 150Oe through the M–H hysteresis loops, and is depicted in Fig. 2(b), which indicates the weak magnetic property. It is also worth mentioning that the as-prepared $BiFeO_3$ powder was attracted to magnetic stir bar easily which was noticed during this experiment. A Nd–Fe–B permanent magnet was applied to prove the magnetic response of the magnetic sample. As shown in the inset of Fig. 2(b), the dark-yellow powders ($BiFeO_3$) can be attracted to the magnet after adsorbing RhB molecules completely, suggesting its potential application in magnetic separation.

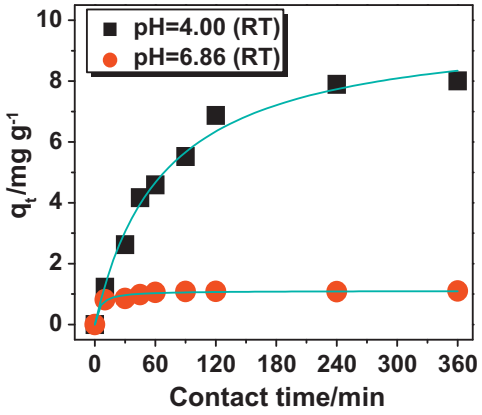

Fig. 3. Time-resolved uptake of RhB onto $BiFeO_3$.

Table 1
Kinetic parameters of the pseudo-second-order model for RhB adsorption on $BiFeO_3$ at different pHs and temperatures.

Adsorption conditions	Pseudo 2nd order kinetic model		
	q_e (mg g^{-1})	k_2 (g mg^{-1} h^{-1})	r^2
pH = 4.00	9.9	14.4	0.99
pH = 6.86	0.3	1.1	0.98
Temperature = 288 K	14.2	120.2	0.95
Temperature = 313 K	10.4	51.8	0.98

RhB molecule is a cationic dye, whose Carboxyl functional groups ($pK_a = 3.0$) [15] could be dissolved in aqueous solution forming a certain faintly acid. In this study, we used the buffer salt to keep the pH of the entire adsorption process stable. The adsorption kinetics study is depicted in Fig. 3, revealed that the adsorption capacity of Rhodamine B on $BiFeO_3$ is quite weak under the neutral pH conditions (pH = 6.86). However, a dramatic increase can be observed by decreasing the pH from 6.86 to 4.00. Meanwhile, the pseudo-second-order adsorption kinetics constant and equilibrium adsorption amount were respectively increased from 0.3 g mg^{-1} h^{-1} and 1.1 mg g^{-1} to 14.4 g mg^{-1} h^{-1} and 9.9 mg g^{-1}, respectively (as shown in Table 1).

In order to study the thermodynamics for the adsorption on $BiFeO_3$, the batch adsorption experiments were conducted in a stirred water bath. Fig. 4 depicts the kinetic adsorption of RhB onto $BiFeO_3$ at different temperatures. It can be noticed clearly that the adsorption capacity of RhB on $BiFeO_3$ is decreased by increasing the adsorption temperature, demonstrating the exothermic nature of the adsorption process. By increasing the adsorption temperature

Table 2
Thermodynamic parameters for the adsorption of RhB on $BiFeO_3$.

Temperature (K)	ΔG° (kJ/mol)	ΔH° (kJ/mol)	ΔS° (J/molK)
288	−9.03	−54.19	−156.8
313	−5.11		

from 288 K to 313 K, the pseudo-second-order adsorption kinetics constant and equilibrium adsorption amount were decreased from 120.2 g mg^{-1} h^{-1} and 14.2 mg g^{-1} to 51.8 g mg^{-1} h^{-1} and 10.4 mg g^{-1} (as listed in Table 1). The change in Gibbs free energy (ΔG) and first law of thermodynamics can be defined and described as below,

$$\Delta G_{abs} = -RT \ \ln K_{abs} \quad (4)$$

$$\Delta G_{abs} = \Delta H_{abs} - T\Delta S_{abs} \quad (5)$$

where R is ideal gas constant (J K^{-1} mol^{-1}), T is absolute temperature (K), K_{abs} is the standard thermodynamic adsorption equilibrium constant defined by $(C_0 - C_e)/C_e$, ΔH_{abs} is the change in enthalpy and ΔS_{abs} is the change in entropy. The thermodynamic parameters ΔG_{abs}, ΔH_{abs} and ΔS_{abs} can be calculated using the mentioned above equations and are listed in Table 2. The obtained negative value of ΔG which demonstrates the adsorption process under such temperature was a spontaneous process. Meanwhile the negative value of ΔH_{abs} and ΔS_{abs} obtained also indicates the exothermic and irreversible characteristic of the adsorption of RhB on $BiFeO_3$ Table 3.

To investigate the saturated adsorption capacity of RhB on $BiFeO_3$ as well the possible mechanism adsorption, the isothermal adsorption behavior of RhB on $BiFeO_3$ at different pH of was studied. As depicted in Fig. 5, it can be seen clearly that initially the saturation adsorption plateau region occurs thus the adsorption isotherms can be better fitted by the Langmuir model than the Freundlich model, implying the possible occurred monolayer adsorption. The saturated adsorption amount of $BiFeO_3$ could be estimated in the 2.5 mg g^{-1} to 11.9 mg g^{-1} range by decrease in pH value from 6.86 to 4.00 as listed in Table 2. The surface zeta potentials of $BiFeO_3$ suspended particle as a function of pHs was studied as well and is presented in Fig. 6. The results showed that $BiFeO_3$ particles surface zeta potential is almost close to zero when the pH is approximately equal to 5.1, indicating that the isoelectrical point of as-prepared $BiFeO_3$ is around 5.1. Therefore, it can be deduced primarily that $BiFeO_3$ surface were positive and negative charged respectively when pH was adjusted to 4.00 and 6.86, revealing the static-electric force adsorption mechanism. This could possibly be occurred between the positive charged $BiFeO_3$ surface (pH = 4.00) and negative charged carboxyl group in RhB molecular (as

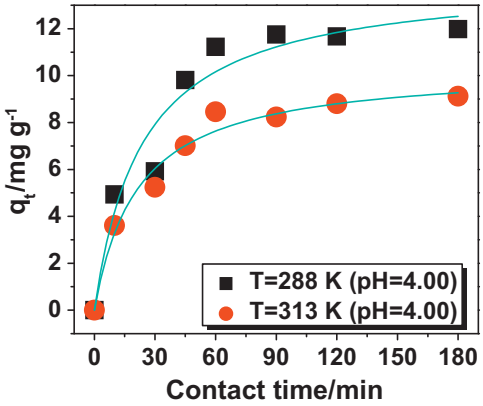

Fig. 4. Dependence of adsorption kinetic of RhB over $BiFeO_3$ at different adsorption temperatures.

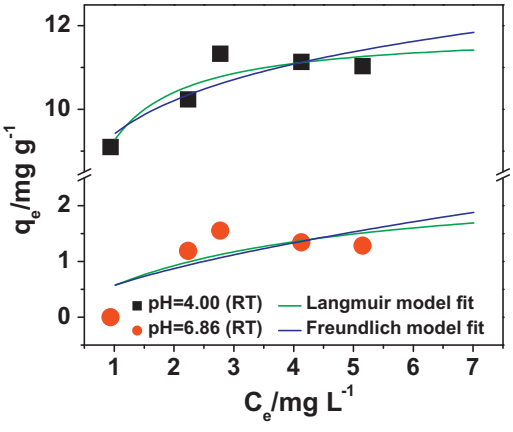

Fig. 5. Dependence of adsorption isotherms of RhB on pH using $BiFeO_3$.

Table 3
Parameters of Langmuir/Freundlich adsorption isothermal models toward RhB molecules on $BiFeO_3$ at room temperature.

pHs	Langmuir model			Freundlich model		
	q_m (mg g^{-1})	K_L (L mg^{-1})	r^2	K_F (mg$^{1-1/n}$ L$^{1/n}$ g^{-1})	n	r^2
pH = 4.00	11.9	3.5	0.87	9.4	8.5	0.78
pH = 6.86	2.5	0.3	0.62	0.6	1.6	0.55

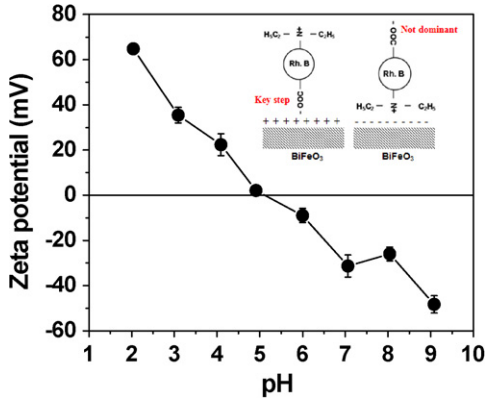

Fig. 6. ζ-Potential of as-prepared $BiFeO_3$ as a function of pH (inset depicts the possible adsorption process trend on $BiFeO_3$ surface).

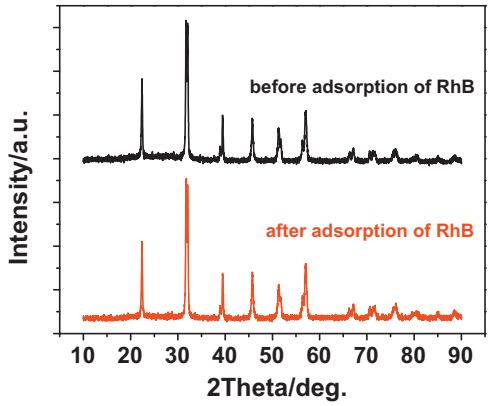

Fig. 7. XRD patterns of $BiFeO_3$ adsorbent before and after adsorption of RhB.

illustrated in the inset of Fig. 6). The high adsorption capacity at pH = 4 (11.9 mg g^{-1} as modeled by Langmuir equation) revealed that the adsorption of RhB on positive charged $BiFeO_3$ surface could be a key process in adsorption. Meanwhile, it is worth noticing that the low adsorption capacity (2.5 mg g^{-1} modeled by Langmuir equation) at pH = 6.86 indicated weak interaction between the negative charged $BiFeO_3$ surface sites and positive charged $-N(Et)_2$ groups. Therefore, the negative charged carboxyl groups of RhB molecules are more likely to be adsorbed onto the positive charged surface of $BiFeO_3$. The RhB dye should not adsorb easily on the surface of negative charged $BiFeO_3$ through positive charged $-N(Et)_2$ groups. The stability of $BiFeO_3$ in water is a significant issue related to the practical applications in water purification. For this purpose, the aqueous suspension of $BiFeO_3$ solid was collected by centrifuging and the XRD patterns of $BiFeO_3$ were recorded before and after irradiation. As depicted in Fig. 7, no apparent change in the XRD patterns was observed after adsorption of RhB at acid conditions of pH = 4.00, suggesting the high stability in the aqueous solution.

It is also worth noticing that our recent results [16,17] demonstate the fact that $BiFeO_3$ based ceremics with dramatically enchaned magnetic properties can be synthesized by doping with transition metal ions such as cobalt and ferric ions. We have demonstrated that the coercivity as high as 500Oe can be reached by doping cobalt ions into $BiFeO_3$ lattices. Therefore, such $BiFeO_3$ based materials with enhanced magnetic property may favor the recycled efficiency. In addition further studies on their adsorption performance are under progress in our group.

4. Conclusions

This paper reports the adsorption removal of RhB molecules on $BiFeO_3$ from aqueous solution for the first time. The sorption isotherm shows that the maximum adsorption capacities of RhB on $BiFeO_3$ can be reached to 11.9 mg g^{-1} when pH of RhB solution was adjusted to 4.00. The results demonstrated that adsorption is of exothermic nature because of the negative value of the enthalpy change (−54.19 kJ/mol). Furthermore the study indicated that the magnetic separable $BiFeO_3$ exhibited excellent adsorption removal performance towards RhB and could possibly be used as a novel adsorbent for waste water treatment contaminated with dyes and other organic pollutants.

Acknowledgements

This work is supported by the National Natural Science Foundation of China (51172044) and the National Science Foundation of Jiangsu Province of China (BK2011617), the Fundamental Research Funds for the Central Universities (NS2012110), National Key Projects for Basic Researches of China (2010CB923404), NCET-09-0296, the Scientific Research Foundation for the Returned Overseas Chinese Scholars, State Education Ministry, and Southeast University (the Excellent Young Teachers Program and Seujq201106).

References

[1] M.C. Tabares, J.F. Rivera, A. Bezinges, A. Monnier, H. Schmid, Jpn. J. Appl. Phy. 1 24 (1985) 1051–1053.
[2] P. Fischer, M. Polomska, I. Sosnowska, M. Szymanksi, J. Phys. C Solid State Phys. 13 (1980) 1931–1940.
[3] J. Wang, J.B. Neaton, H. Zheng, V. Nagarajan, S.B. Ogale, B. Liu, D. Viehland, V. Vaithyanathan, D.G. Schlom, U.V. Waghmare, N.A. Spaldin, K.M. Rabe, M. Wuttig, R. Ramesh, Science 299 (2003) 1719–1722.
[4] W. Eerenstein, F.D. Morrison, J.M. Dho, G. Blamire, J.F. Scott, N.D. Mathur, Science 307 (2005), 1203–1203.
[5] K. Takahashi, N. Kida, M. Tonouchi, Phys. Rev. Lett. 97 (2006) 240403.
[6] Q.Y. Xu, X.H. Zheng, Z. Wen, Y. Yang, D. Wu, M.X. Xu, Solid State Commun. 151 (2011) 624–627.
[7] F. Gao, X. Chen, K. Yin, S. Dong, Z. Ren, F. Yuan, T. Yu, Z. Zou, J.M. Liu, Adv. Mater. 19 (2007) 2889–2892.
[8] X.M. Lu, J.M. Xie, Y.Z. Song, J.M. Lin, J. Mater. Sci. 42 (2007) 6824–6827.
[9] Y.N. Huo, Y. Jin, Y. Zhang, J. Mol. Catal. A: Chem. 331 (2010) 15–20.
[10] X. Xu, Y.H. Lin, P. Li, L. Shu, C.W. Nan, J. Am. Ceram. Soc. 94 (2011) 2296–2299.
[11] X. Wang, Y. Lin, X.F. Ding, J.G. Jiang, J. Alloys Compd. 509 (2011) 6585–6588.
[12] W. Luo, L.H. Zhu, N. Wang, H.Q. Tang, M.J. Cao, Y.B. She, Environ. Sci. Technol. 44 (2010) 1786–1791.
[13] A. Özcan, E.M. Öncü, A.S. Özcan, Colloids Surf., A 277 (2006) 90–97.
[14] O. Hamdaoui, E. Naffrechoux, J. Hazard. Mater. 147 (2007) 381–394.
[15] G.J. Mohr, F. Lehmann, U.W. Grummt, U.E. Spichiger, Anal. Chim. Acta 344 (1997) 215–225.
[16] Q. Xu, H.F. Zai, D. Wu, T. Qiu, M.X. Xu, Appl. Phys. Lett. 95 (2009) 112510.
[17] X.H. Zheng, Q.Y. Xu, Z. Wen, X.Z. Lang, D. Wu, T. Qiu, M.X. Xu, J. Alloys Compd. 499 (2010) 108–112.